

Enhancing Instruction-Following Capability of Visual-Language Models by Reducing Image Redundancy

Te Yang^{1,2}, Jian Jia³, Xiangyu Zhu^{1,2}, Weisong Zhao⁴, Bo Wang³, Yanhua Cheng³, Yan Li³, Shengyuan Liu², Quan Chen³, Peng Jiang³, Kun Gai³, Zhen Lei^{1,2,5}

¹State Key Laboratory of Multimodal Artificial Intelligence Systems, Institute of Automation, Chinese Academy of Sciences

²School of Artificial Intelligence, University of Chinese Academy of Sciences, Beijing, China

³Kuaishou Technology

⁴School of Cyber Security, University of Chinese Academy of Sciences, Beijing, China

⁵CAIR, HKISI, Chinese Academy of Sciences

{yangte2021, xiangyu.zhu, zhen.lei}@ia.ac.cn, jian.jia@outlook.com, zhaoweisong@iie.ac.cn, wangbo0060@163.com, chengyanhua@kuaishou.com, yan.li@cripac.ia.ac.cn, myctllmail@163.com, jp2006@139.com, kun.gai@qq.com

Abstract

Large Language Models (LLMs) have strong instruction-following capability to interpret and execute tasks as directed by human commands. Multimodal Large Language Models (MLLMs) have inferior instruction-following ability compared to LLMs. However, there is a significant gap in the instruction-following capabilities between the MLLMs and LLMs. In this study, we conduct a pilot experiment, which demonstrates that spatially down-sampling visual tokens significantly enhances the instruction-following capability of MLLMs. This is attributed to the substantial redundancy in visual modality. However, this intuitive method severely impairs the MLLM’s multimodal understanding capability. In this paper, we propose Visual-Modality Token Compression (VMTC) and Cross-Modality Attention Inhibition (CMAI) strategies to alleviate this gap between MLLMs and LLMs by inhibiting the influence of irrelevant visual tokens during content generation, increasing the instruction-following ability of the MLLMs while retaining their multimodal understanding capacity. In VMTC module, the primary tokens are retained and the redundant tokens are condensed by token clustering and merging. In CMAI process, we aggregate text-to-image attentions by text-to-text attentions to obtain a text-to-image focus score. Attention inhibition is performed on the text-image token pairs with low scores. Our comprehensive experiments over instruction-following capabilities and VQA-V2 (Goyal et al. 2017), GQA (Hudson and Manning 2019), TextVQA (Singh et al. 2019), MME (Fu et al. 2024) and MMBench (Liu et al. 2023a) five benchmarks, demonstrate that proposed strategy significantly enhances the instruction following capability of MLLMs while preserving the ability to understand and process multimodal inputs.

Introduction

Achieving alignment between artificial intelligence systems and human intentions has long been an important objective in AI research (Ji et al. 2023; Han et al. 2022). It ensures that the behavior and decision making of AI systems are consistent with human intentions and values, thereby ensuring that the development and application of AI are beneficial and

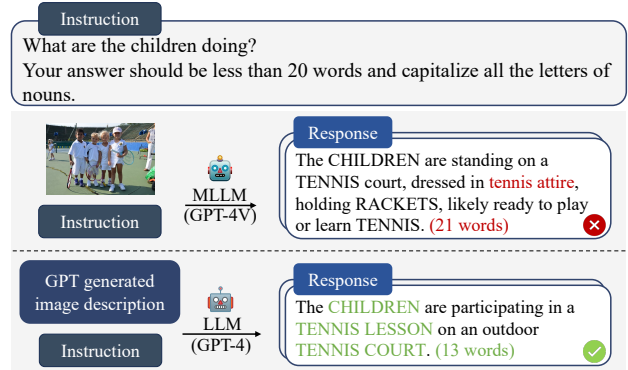


Figure 1: Illustration of the gap in the instruction-following ability between GPT4 (Achiam et al. 2023) and GPT-4V (OpenAI 2023). Under the same instruction, GPT-4V cannot generate outputs that meet the requirements of the instruction. However, when the image in the input is replaced with a detailed description of the image generated by GPT-4, the model can correctly follow the provided instructions.

pose no harm to humans. Ensuring that machines can precisely follow human instructions is a preliminary yet crucial step in achieving this alignment.

Large language models (LLMs) have been significantly improved owing to innovations in model architecture and large-scale pre-training (Achiam et al. 2023; Touvron et al. 2023b), resulting in accurate responses to complex human instructions. Despite the significant progress in MLLMs driven by advancements in LLMs, there is a substantial gap between MLLMs and their foundations LLMs regarding precise instruction-following ability. Replacing multimodal inputs with text-only inputs significantly increases the instruction-following capabilities of MLLMs (Figure 1). This phenomenon is common and cannot be avoided even in the best closed-source MLLMs.

This gap prompts our investigation into the instruction-following capability of MLLMs. As discussed in (He et al. 2022), one significant difference between the vision modality and the language modality is the extent of information redundancy. Language is a medium of human communication with a low information redundancy and rich semantics.

Conversely, images are highly spatially redundant. Notably, masked image modeling can adopt a significantly larger masking ratio, reaching 90%, compared to language (He et al. 2022). Therefore, it is imperative to explore whether reducing the redundant information in images can enhance the instruction-following capabilities of MLLMs.

Conventional MLLMs generally adhere to a design paradigm comprising two stages: visual-modality processing and cross-modality content generation. In the former stage, images are tokenized using a visual encoder with an adapter. In the cross-modality content generation stage, the LLM produces the desired output using visual tokens and text embeddings as inputs. Consequently, we formulate two research questions: 1) How can we reduce the redundancy in visual modality? 2) How can we minimize the impact of redundancy in visual modality on the cross-modality content generation process?

The instruction-following capabilities of MLLMs can be significantly improved by reducing redundant information in images using an intuitive spatial down-sampling strategy over visual tokens. However, this simple strategy significantly impairs visual understanding capabilities of MLLMs. In this study, we utilize 1) visual-modality token compression (VMTC) and 2) cross-modality attention inhibition (CMAI) to address those two above-mentioned problems, respectively. The VMTC module is designed to compress redundant information of images while retaining the critical foreground information. It leverages attention scores in the ViT layers to identify redundant background tokens, which are clustered based on token similarity and fused accordingly. The CMAI module is presented to mitigate the impact of visual redundancy by ensuring that each text token in the LLM concentrates exclusively on the relevant image tokens. This is achieved by attenuating the attention level between text-image token pairs with low text-to-image focus scores. The comprehensive experimental results demonstrate that our method achieves SOTA performance on instruction-following capabilities while precisely maintaining the multimodal understanding capabilities of MLLMs. The major contributions of this study are summarized as below:

- To the best of our knowledge, this is the first study to investigate the instruction-following capability of MLLMs from a model perspective and propose a correlation between the instruction-following capability of MLLMs and the redundancy of visual modality.
- We propose visual-modality token compression strategy to compress redundant visual information and cross-modality attention inhibition approach to reduce the impact of visual redundancy on text generation.
- By integrating VMTC and CMAI, our method significantly improves the instruction-following capabilities of MLLMs, while precisely maintaining the performance of the baseline model.

Related Work

Multimodal Large Language Models. Benefiting from recent advancements of LLMs (Achiam et al. 2023; Touvron et al. 2023a,b), multimodal large language models have

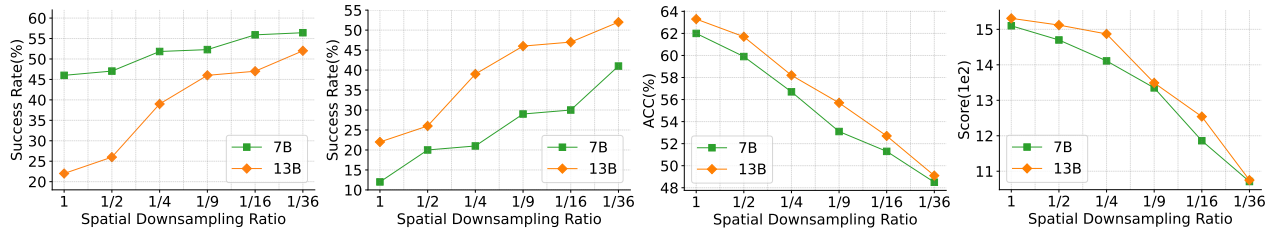
demonstrated remarkable capabilities across various visual-language tasks (Li et al. 2023b; Alayrac et al. 2022; Dai et al. 2023; Liu et al. 2024b). BLIP2 and InstructBLIP (Li et al. 2023b; Dai et al. 2023) employ the Q-Former to aggregate visual features and LLaVA (Liu et al. 2024b) uses a linear projection layer to align the token dimensions of the visual encoder with LLM. These methods significantly enhancing the model’s ability to interpret and understand images. Many works continue to explore this area from different directions, including adopting higher image resolutions (Lin et al. 2023b; Li et al. 2023a; Xu et al. 2024), efficient MLLMs (Chu et al. 2024), and extending applications to the video domain (Lin et al. 2023a; Kim et al. 2024).

Token Pruning. Researchers have proposed various approaches (Rao et al. 2021; Wei et al. 2023; Bolya et al. 2023) to remove redundant tokens in ViT (Dosovitskiy et al. 2020) to improve the model’s computational efficiency. Meanwhile, many works (Cao et al. 2024; Cao, Paranjape, and Hajishirzi 2023; Wang et al. 2023) have improved the computational efficiency of visual-language models through pruning, but these efforts have primarily focused on traditional VLMs (Li et al. 2022; Radford et al. 2021). Recently, LLaVA-Prunerge (Shang et al. 2024) proposes to reduce visual tokens in last hidden layer of ViT. However, this work also aims to enhance the computational efficiency of MLLMs, while our focus is on improving the instruction-following capability of MLLMs.

Instruction-Following. A series of works have been proposed to address the instruction-following capability of large language models, including human evaluation (Ouyang et al. 2022; Zheng et al. 2024; Taori et al. 2023), model-based evaluation (Chang et al. 2023; Liu et al. 2023b), and evaluation based on quantitative benchmarks (Koubaa 2023; Katz et al. 2024; Chang et al. 2023). In particular, IFEval (Zhou et al. 2023) introduces instruction-following evaluation based on verifiable instructions, which can automate the evaluation process and enhances the accuracy and consistency of the evaluation process. In the context of multimodal large models, most works (Li et al. 2023c; Luo et al. 2023; Liu et al. 2024b) start from a data perspective, constructing instruction datasets to enable models to acquire instruction-following capability. In our study, we investigate the factors influencing the instruction-following capability of MLLMs and enhance the model’s instruction-following capability from a model architecture perspective.

Pilot Studies

We conduct pilot experiments on the instruction following abilities of existing MLLMs, using GPT-4V (OpenAI 2023) and LLaVA-1.5 (Liu et al. 2024a) as representative models. Developed and maintained by OpenAI, GPT-4V is one of the most advanced proprietary LLM. Currently, LLaVA-1.5 is one of the most impactful open-source MLLMs available. GPT-4V has a proprietary nature, thus we use case studies to evaluate its instruction-following capabilities. We manually design instructions and use them as input with a related image to assess the ability of GPT-4V model to generate accurate responses. GPT-4V is also used to generate descriptions of images. Subsequently, these descrip-



(a) Instruction following performance on JSON task . (b) Instruction following performance on keywords task (c) Multimodal understanding capability on GQA benchmark. (d) Multimodal understanding capability on MME benchmark.

Figure 2: Illustration of instruction following performance and multimodal understanding capability of LLaVA-1.5 using different spatial down-sampling ratio. In Figure 2a and 2b, the instruction-following performances are significantly improved as the down-sampling ratio increases. In Figure 2c and 2d, down-sampling operations significantly affect the model’s multimodal understanding capability.

tions are used as input along with the instructions to evaluate the instruction-following capabilities of GPT-4 model, as a control. The findings demonstrated a significant gap in instruction-following capabilities between GPT-4V and GPT-4 models as shown in Figure 1. More examples are presented in the appendix.

Such gap prompts us to explore the differences between visual modality and language modality. Images are unstructured information with a high degree of spatial redundancy. Conversely, text is highly structured information with low redundancy. As illustrated in (He et al. 2022; Wettig et al. 2022), when the mask ratio exceeds 80%, the accuracy loss in masked image modeling methods is negligible (0.5%), compared to the optimal ratio. In contrast, masked language modeling methods exhibit a significant degradation in accuracy (over 10%) under similar conditions. This disparity indicates the differences in information redundancy between language and images. We hypothesize that reducing redundancy in images can improve the instruction-following ability of multimodal large language models.

We conduct experiments using LLaVA-1.5 (Liu et al. 2024a) 7B and 13B models. In the pilot experiments, we conduct spatial down-sampling of the tokens obtained from the image encoded by ViT to reduce image redundancy. We evaluate the model’s instruction-following capability based on its ability to perform two simple tasks: responding in JSON format and including specific keywords in the answers. The results of the model’s instruction-following capability and multimodal understanding capability under different spatial down-sampling ratios are shown in Figure 2. The results indicate that an increase in the spatial down-sampling ratio reduces the redundancy in the images, leading to a significant enhancement of the model’s instruction-following capabilities (Figure 2a and Figure 2b). However, the results also demonstrate that the straightforward strategy of spatial down-sampling significantly impairs the model’s multimodal understanding capabilities (Figure 2c and Figure 2d). This finding prompts us to explore more optimal solutions that enhance the instruction-following capabilities of MLLMs without substantially compromising its inherent multimodal understanding capabilities.

Method

The enhancement of instruction-following capability in MLLMs through the reduction of redundant information via spatial down-sampling in images has been previously discussed. However, this approach significantly compromises the model’s multimodal understanding ability. Our objective is to improve the instruction-following capability of MLLMs while preserving their multimodal understanding abilities. Figure 3 illustrates an overview of our proposed model architecture. This section begins with an introduction to MLLMs. The Visual-Modality Token Compression (VMTC) method is then elucidated. This technique preserves crucial foreground information while compressing less significant background details. Finally, the Cross-Modality Attention Inhibition (CMAI) is presented. CMAI is designed to mitigate the impact of redundant image information on text generation.

Preliminary

MLLMs typically process both image and text inputs, generating textual responses as output. The current predominant architecture of MLLMs generally comprises three key components: a visual encoder, a projection layer, and a LLM. The visual encoder E , typically employing the Vision Transformer (ViT) (Dosovitskiy et al. 2020) architecture, consists of multiple stacked transformer blocks. These blocks transform input image patches I to visual tokens T . Each transformer block is composed of Multi-head Self-attention (MSA) and Feed-forward Layer components.

$$z'_l = \text{MSA}(z_{l-1}) + z_{l-1}, \quad (1)$$

$$z_l = \text{MLP}(z'_l) + z'_l, \quad (2)$$

where z_{l-1} and z_l are hidden states in $l - 1$ th and l th layer. The projection layer $Proj$ is designed to align the dimensions of visual tokens with the input dimensions of the LLM.

$$T' = Proj(T). \quad (3)$$

As a result, the dimension of $T' \in \mathbb{R}^{n \times d}$ is aligned with the LLM. The input of LLM consists aligned image tokens T' and text X_q , and the output are the textual tokens X_a . The LLM also adopts the transformer architecture (Vaswani 2017) but are typically with causal attention masks to ensure

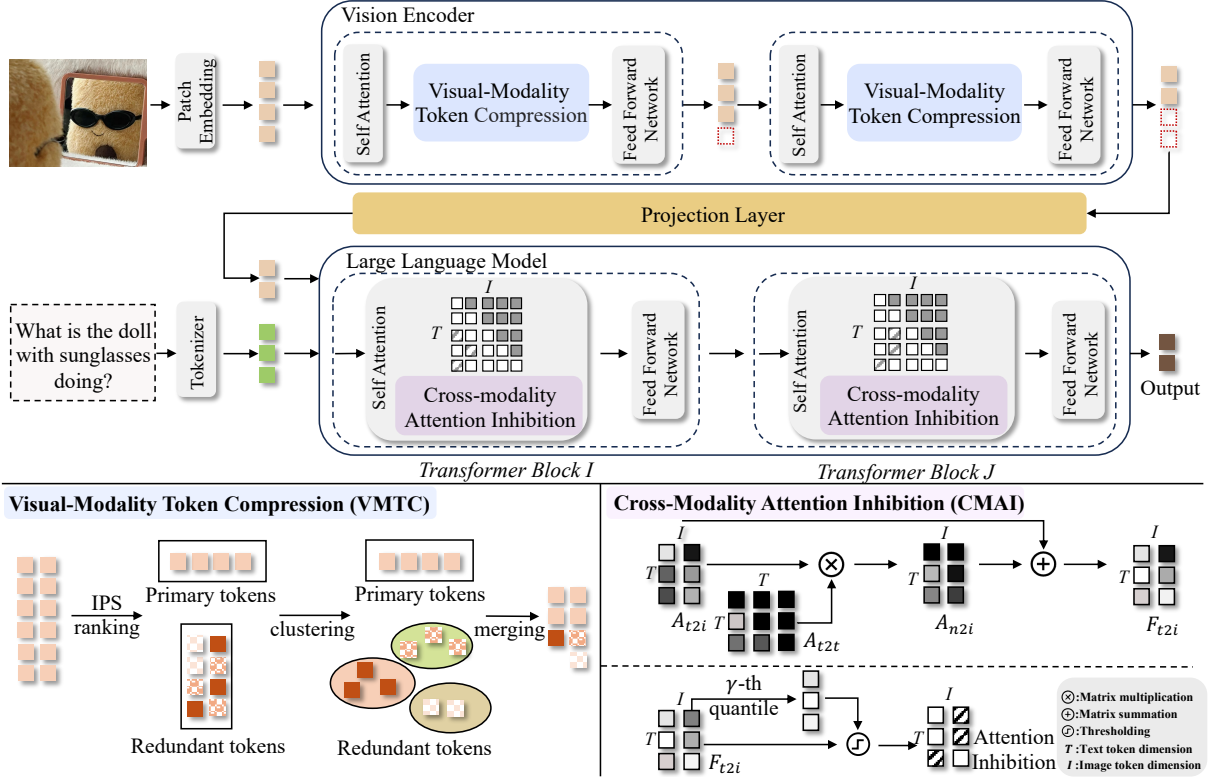


Figure 3: Overview of our proposed framework. Our proposed framework incorporates two principal components: the VMTC module and the CMAI module. The VMTC module is strategically positioned within several transformer blocks of the visual encoder, specifically between the self-attention and feed-forward networks. This module aims to compress image redundancy by retaining primary tokens while clustering and merging redundant tokens. Meanwhile, the CMAI module is integrated into the self-attention modules of transformer blocks in LLMs, effectively inhibiting the influence of redundant image tokens.

no information leakage occurs during text generation.

$$\text{SelfAttn}(Q, K, V) = (\text{softmax}(\frac{QK^T}{\sqrt{d_k}}) + M)V, \quad (4)$$

where Q, K, V are different projections of the hidden state z_l , and M is the causal attention mask which has negative infinity above the diagonal and zeros in all other positions. QK^T is referred to as the attention score, while the result of this expression $\text{softmax}(\frac{QK^T}{\sqrt{d_k}})$ is the attention weights.

Visual-Modality Token Compression

In order to compress spatially redundant information in images and enhance the model’s instruction-following capability, we implement a strategy that preserves essential foreground tokens while clusters and merges the remaining ones. This approach is based on researches (Wei et al. 2023) indicating that the complete elimination of remaining tokens can have an adverse effect on model performance. Specifically, given the average attention weight of different attention heads $A_w \in \mathbb{R}^{(n+1) \times (n+1)}$, we define the attention weights between each patch token $\{z_l^1, \dots, z_l^n\}$ and class token $\{z_l^0\}$ as importance score $\text{IPS} \in \mathbb{R}^n$. Supposing the number of output tokens is $k + 1 + c$, where c is the clustering number, the class token $\{z_l^0\}$ and the top k patch tokens with the highest importance scores IPS are selected as

primary tokens $z_{l,kp}^i$ and other tokens are considered as redundant tokens $z_{l,rd}^j$:

$$z_{l,kp}^i = \{z_l^i | \text{rank}(\text{IPS}(i)) \leq k, 1 \leq i \leq n\}. \quad (5)$$

$$z_{l,rd}^j = \{z_l^j | \text{rank}(\text{IPS}(j)) > k, 1 \leq j \leq n\}. \quad (6)$$

To effectively preserve information from redundant tokens while minimizing image redundancy, a token merging strategy is employed. Given that redundant tokens may belong to diverse semantic categories, indiscriminate merging could lead to semantic confusion. To address this challenge, the K-Means algorithm is utilized to cluster tokens based on cosine similarity. Within each cluster $\{C_1, \dots, C_s\}$, tokens are considered semantically similar and are merged based on IPS. This approach enables the compression of redundant information while maintaining the semantic integrity of the image content.

$$z_{l,C_i}^j = \sum_{\{j | z_l^j \in z_{l,rd}^j, z_l^j \in C_i\}} \text{IPS}(j) z_l^j. \quad (7)$$

Finally, the intermediate representation of z_l^i is updated as:

$$z_l^i = \text{cat}(z_l^0, z_{l,kp}^i, z_{l,C_1}^i, \dots, z_{l,C_s}^i). \quad (8)$$

Cross-Modality Attention Inhibition

Despite the compression of image redundancy in the visual modality, retaining an insufficient number of tokens can sig-

nificantly impair the model’s multimodal understanding capability. To address this issue, we propose cross-modality attention inhibition, a plug-and-play module for Large Language Models (LLMs). This module enables each text token to focus exclusively on the most relevant image tokens, thereby mitigating the impact of redundant information.

Given a sequence of tokens $\{I_1, \dots, I_n, T_1, \dots, T_m\}$, where I and T represent image and text tokens, respectively, and an average attention score $A_s \in \mathbb{R}^{(n+m) \times (n+m)}$, we define text-to-image attentions $A_{t2i} \in \mathbb{R}^{m \times n} \subset A_s$ as elements where the queries are text tokens and the keys are image tokens. Similarly, text-to-text attentions $A_{t2t} \in \mathbb{R}^{m \times m} \subset A_s$ are defined as elements where both the query and the key are text tokens. The primary objective is to effectively identify and suppress incorrect associations between image and text tokens, ensuring the preservation of only relevant connections. To achieve this goal, we consider not only each text token’s own attentiveness to image tokens, but also the attention of other text tokens it attends to. We use the neighborhood text-to-image attention A_{n2i} to quantify this attentiveness, aggregating A_{t2i} through neighborhood text-to-text attention A_{t2n} . The neighborhood text-to-text attention serves to quantify a text token’s focus on neighboring tokens, excluding itself. Finally, we combine A_{n2i} and A_{t2i} to obtain the text-to-image focus score F_{t2i} .

$$A_{t2n}^{jk} = \begin{cases} A_{t2t}^{jk}, & \text{if } j > k, \\ 0, & \text{if } j \leq k, \end{cases} \quad (9)$$

$$A_{n2i}^{jk} = \sum_{h \in \{1, \dots, m\}} A_{t2n}^{jh} A_{t2i}^{hk}, \quad (10)$$

$$F_{t2i} = A_{n2i} + A_{t2i}, \quad (11)$$

where j, k denote the row and column indices, respectively. Conceptually, if a text token allocates greater attention to another particular text token, then the focus of that particular text token on image tokens should be weighted more prominently in A_{n2i} . Finally, given attention inhibition ratio γ , we calculate γ -th quantile for each row of F_{t2i} as thresholds. Then we perform attention inhibition on text-image token pairs with F_{t2i} below these thresholds by adding negative infinities on causal masks at corresponding positions.

Experiments

Experimental Settings

Implementation Details. In this study, CLIP-ViT-L/14 (Radford et al. 2021) is employed as the image encoder. The projection layer consists of a two-layer MLP with a GELU (Hendrycks and Gimpel 2016) activation function. Vicuna-v1.5 (Chiang et al. 2023) is selected as the large language model. The VMTC module is inserted into equally spaced transformer blocks to achieve a total token compression ratio of 50%, unless otherwise specified. The CMAI module is incorporated into all layers of the LLM, applying a linearly increasing attention inhibition ratio with a maximum of 60%. Datasets and training configurations are adopted following LLaVA-1.5 (Liu et al. 2024a) in both the pretraining and instruction tuning stages.

Evaluation. Five widely-recognized benchmarks are utilized to evaluate the model’s performance. Three academic-task-oriented benchmarks are employed: VQA-V2 (Goyal et al. 2017) and GQA (Hudson and Manning 2019) assess visual perception capabilities through open-ended visual question answering, while TextVQA (Singh et al. 2019) examines the ability to answer OCR-based visual questions. Additionally, two comprehensive datasets, MME (Fu et al. 2024) and MMBench (Liu et al. 2023a), are used to provide a thorough evaluation of the model. To evaluate instruction-following capabilities, MLLMs are required to perform 16 different verifiable instruction-following tasks (Zhou et al. 2023) while answering image-related questions. The success rates of these tasks are reported. The selected tasks are achievable yet challenging for MLLMs and are categorized into five groups:

- Text formatting (T1-3): Remove Commas, Lowercase Conversion and Uppercase Conversion.
- Including required content: Placeholder, Postscript, Title and Keyword.
- Specific format (T8-11): Add Highlights, JSON Format, Answer in Sections and Answer in Bullet Points.
- Length Limit(T12-13): Sentence Count and Word Count.
- Other(T14-16): Dual Response Combination, Ending Constraint and Starting Constraint.

Comparison Experiments

Comparison of Instruction-Following Capability. A comparison of instruction-following capabilities and multimodal understanding capability, as measured by performance on GQA (Hudson and Manning 2019), is conducted between LLaVA-1.5 (Liu et al. 2024a), spatially down-sampled LLaVA-1.5, and the proposed model. The results are presented in Table 1. Furthermore, experiments are conducted where the model first describes an image in text and then completes text-only instruction-following tasks, serving as an upper limit for the instruction-following tasks. Spatial down-sampling, as an intuitive solution to improve instruction-following capability, yields 3.7% and 5.3% improvements in success rates for LLaVA-1.5 7B and 13B. However, this approach is not ideal due to significant performance degradations over GQA of -2.1% and -1.6%.

In contrast, the proposed method enhances the instruction-following capabilities of LLaVA-1.5 by up to 9.4% and 9.5% with minimal performance loss of -0.4% and 0% on GQA, significantly outperforming the spatial downsampling strategy.

The gap of 5.5% and 6.5% remains compared to the upper limits, highlighting the disparity between MLLMs and LLMs in instruction-following. However, it is important to note that the upper-limit method can severely impair multimodal understanding due to the information loss that occurs between the two stages.

Comparison with the SOTA Methods. To demonstrate the efficacy of our approach, we conduct a comparative analysis against leading MLLMs, including Shikra (Chen et al. 2023b), IDEFICS (IDEFICS 2023), Qwen-VL (Bai et al.

Method	GQA	T1	T2	T3	T4	T5	T6	T7	T8	T9	T10	T11	T12	T13	T14	T15	T16	AVG
LLaVA-1.5-7B	62.0	57.3	06.0	39.9	16.1	40.4	53.2	21.1	06.4	45.4	54.1	26.6	56.4	51.4	01.8	11.0	67.4	34.7
LLaVA-1.5-13B	63.3	53.7	46.8	35.8	14.2	62.8	72.0	12.4	02.8	21.6	83.0	56.4	65.1	50.0	20.2	19.7	57.8	42.1
SPD-7B	59.9	56.9	07.3	46.8	17.9	41.7	63.8	22.0	08.3	47.7	56.0	35.8	63.8	54.1	02.8	15.1	73.9	38.4
SPD-13B	61.7	58.7	58.7	51.8	20.6	63.3	75.2	15.1	01.8	28.0	83.0	70.2	64.7	52.8	13.8	33.9	67.4	47.4
Upper Limit-7B	48.52	35.8	01.4	38.1	33.9	68.4	80.7	33.9	10.1	68.8	90.8	62.4	66.1	53.7	07.8	42.2	100.0	49.6
Upper Limit-13B	48.68	49.5	83.9	76.2	12.8	79.8	38.1	33.5	04.1	77.1	89.0	69.7	76.6	60.1	02.8	79.4	96.3	58.1
Ours-7B	61.6	63.3	09.6	60.6	21.6	47.3	64.7	23.4	12.4	54.6	72.9	42.2	69.7	60.6	03.2	18.4	81.2	44.1
Ours-13B	63.3	63.8	62.8	69.3	21.0	65.1	83.0	13.8	03.7	28.4	85.3	74.8	71.6	56.9	20.6	37.2	68.8	51.6

Table 1: Comparison experimental results of Instruction Following Capabilities and GQA (Hudson and Manning 2019). The SPD method refers to the spatial down-sampling version of LLaVA-1.5 (Liu et al. 2024a).

Method	LLM	Image Size	Sample Size Pretrain	Sample Size Finetune	IF \uparrow	VQAv2 \uparrow	GQA \uparrow	TextVQA \uparrow	MME \uparrow	MMB \uparrow
Shikra (Chen et al. 2023b)	Vicuna-13B	224 ²	600K	5.5M	–	77.4	–	–	–	58.8
IDEFICS-9B (IDEFICS 2023)	LLaMA-7B	224 ²	353M	1M	18.9	50.9	38.4	25.9	–	48.2
IDEFICS-80B (IDEFICS 2023)	LLaMA-65B	224 ²	353M	1M	–	60.0	45.2	30.9	–	54.5
Qwen-VL (Bai et al. 2023)	Qwen-7B	448 ²	1.4B	50M	14.7	78.8	59.3	63.8	–	38.2
Qwen-VL-Chat (Bai et al. 2023)	Qwen-7B	448 ²	1.4B	50M	35.0	78.2	57.5	61.5	1487.5	60.6
MiniGPT-v2 (Chen et al. 2023a)	LLaMA2-7B	448 ²	–	–	19.4	–	60.1	–	–	–
SPHINX (Lin et al. 2023b)	LLaMA-13B	448 ²	1.0B	–	23.1	78.1	62.6	51.6	1476.1	66.9
OtterHD-8B (Li et al. 2023a)	Fuyu-8B	1024 ²	–	–	–	–	–	–	1294	58.3
mPLUG-Owl2 (Yu et al. 2024)	LLaMA-7B	448 ²	400M	1.2M	36.8	79.4	56.1	54.3	1450.2	64.5
LLava-1.5-7B(Liu et al. 2024a)	Vicuna-7B	336 ²	558K	665K	34.7	78.5	62.0	58.2	1510.7	64.3
LLava-1.5-13B(Liu et al. 2024a)	Vicuna-13B	336 ²	558K	665K	42.1	80.0	63.3	61.3	<u>1531.3</u>	67.7
Ours-7B	Vicuna-7B	336 ²	558K	665K	<u>44.1</u>	78.4	61.6	57.8	1518.5	66.1
Ours-13B	Vicuna-13B	336 ²	558K	665K	51.6	79.1	63.3	<u>58.6</u>	1548.7	<u>67.5</u>
#Visual Tokens: 64										
InstructBLIP (Dai et al. 2023)	Vicuna-7B	224 ²	129M	1.2M	17.1	–	49.2	50.1	–	36
InstructBLIP (Dai et al. 2023)	Vicuna-13B	224 ²	129M	1.2M	20.7	–	49.5	50.7	1212.8	–
Ours-7B	Vicuna-7B	336 ²	558K	665K	<u>45.4</u>	<u>76.1</u>	<u>58.6</u>	<u>55.9</u>	<u>1468.3</u>	<u>63.0</u>
Ours-13B	Vicuna-13B	336 ²	558K	665K	52.5	77.2	60.2	58.2	1508.6	66.0
#Visual Tokens: 36										
BLIP-2 (Li et al. 2023b)	Vicuna-13B	224 ²	129M	–	–	65.0	41	42.5	1293.8	–
LLaVA-Prumerge (Shang et al. 2024)	Vicuna-7B	336 ²	558K	665K	45.8	72.0	–	–	1350.3	60.9
LLaVA-Prumerge (Shang et al. 2024)	Vicuna-13B	336 ²	558K	665K	<u>52.8</u>	<u>72.8</u>	–	–	<u>1428.2</u>	62.3
Ours-7B	Vicuna-7B	336 ²	558K	665K	47.0	<u>73.9</u>	<u>56.9</u>	<u>54.1</u>	1418.2	<u>62.7</u>
Ours-13B	Vicuna-13B	336 ²	558K	665K	53.5	75.1	57.8	56.9	1452.9	63.9

Table 2: Comparison experiments with the state-of-the-art methods over instruction following capabilities (IF) and five popular MLLM benchmarks.

2023), MiniGPT-v2 (Chen et al. 2023a), SPHINX (Lin et al. 2023b), OtterHD-8B (Li et al. 2023a), mPLUG-Owl2 (Yu et al. 2024) and LLaVA-1.5 (Liu et al. 2024a) (Table 2). Qualitative outcomes are illustrated in Figure 4.

The experimental results reveal that our model’s instruction-following capability significantly surpasses that of other models. Our model exhibits minimal performance degradation compared to LLaVA-1.5 in terms of multimodal understanding capability. The 7B version incurs marginal losses of only -0.1, -0.4, and -0.4 on the VQA-V2, GQA, and TextVQA datasets, respectively. Moreover, it achieves substantial performance gains of 7.8 and 1.8 on MME and MMBench.

The 13B model maintains or exceeds LLaVA-1.5’s performance on most datasets, with the exception of TextVQA. This discrepancy is attributed to the prevalence of optical characters in the background of images in many TextVQA examples, which are compressed and inhibited as redundant information in our approach. To further validate our approach’s effectiveness, we present our model’s performance

while retaining fewer visual tokens and compare it with models utilizing similar visual token numbers. The results demonstrate that our method significantly outperforms InstructBlip (Dai et al. 2023) and LLaVA-Prumerge (Shang et al. 2024) in both instruction following and multimodal understanding capabilities. This underscores our model’s proficiency in compressing and suppressing redundant information while preserving essential image details.

Ablation Studies

Impact of Proposed Modules. As illustrated in Table 3, substantial improvements in instruction following capability are attributed to both visual-modality token compression and cross-modality attention inhibition, which minimally affect the model’s multimodal understanding capability. The individual adoption of these techniques results in performance improvements of 5.2% and 3.9% for success rates in instruction following tasks, respectively. When simultaneously employed, these techniques enhance performance by 9.5%. Concurrently, the accuracy on the GQA benchmark

Instruction: How's the weather? At the end of your response, please explicitly add a postscript starting with P.S.



InstructBlip: sunny (No P.S)

Qwen-VL: It's a sunny day in Portland, Oregon. (No P.S)

SPHINX: Sunny (No P.S)

mPLUG-Owl2: The weather is clear and sunny. (No P.S)

MiniGPT-v2: The skyline in the image is very impressive and looks like a modern city. There are tall buildings with glass facades, some of which appear to be office buildings or residential apartments. The water in the foreground looks calm and there are boats moored near the shore. The weather seems clear and sunny, with blue skies and puffy clouds. (No P.S)

LLaVA-1.5: The weather is sunny and clear, making it a perfect day for sightseeing and enjoying the city's skyline. (No P.S)

IDEFICS: Hi there! I hope you are doing well today :) The current temperature in Portland is around seventy degrees Fahrenheit and it looks like we will have partly cloudy skies throughout most parts of this weekend (PPS - make sure to check out our local forecast for any changes).

Ours: The weather appears to be clear and sunny in the image, making it a beautiful day for sightseeing.

P.S. The presence of multiple boats in the water suggests that the area might be a popular spot for boating activities or tourism.

Figure 4: Qualitative results of instruction following capabilities, comparing our proposed method with InstructBlip (Dai et al. 2023), IDEFICS (IDEFICS 2023), Qwen-VL (Bai et al. 2023), MiniGPT-v2 (Chen et al. 2023a), SPHINX (Lin et al. 2023b), mPLUG-Owl2 (Yu et al. 2024) and LLaVA-1.5 (Liu et al. 2024a).

VMTC	CMAI	GQA	TQA	MME	IF
✗	✗	62.0	58.2	1510.7	34.7
✓		61.7	57.9	1508.9	<u>39.9</u>
	✓	<u>61.9</u>	<u>58.1</u>	1518.5	38.6
✓	✓	61.6	57.8	<u>1515.8</u>	44.2

Table 3: Ablation study of the proposed methodologies, where VMTC denotes Visual-Modality Token Compression and CMAI represents Cross-Modality Attention Inhibition. (TQA: TextVQA)

exhibits only slight decreases of 0.3% and 0.1%. These findings demonstrate that our method effectively preserves the model’s ability to capture essential visual information while compressing and suppressing redundant data.

Impact of Different Stages in Visual-Modality Token Compression. Table 4 elucidates the effects of various stages in visual-modality token compression. A comparative analysis is conducted between the method of pruning solely in the hidden states of last layer, as employed in LLaVA-Prumerge, and our proposed multi-stage approach. The results indicate that pruning exclusively in the final layer leads to significant performance degradation. Conversely, distributing the pruning process across multiple intermediate layers yields comprehensive improvements in both multimodal understanding and instruction-following capabilities. The merging of redundant tokens into a single entity, which mitigates information loss, results in an additional performance increase of 0.4% in both the GQA benchmark and instruction-following capability. Furthermore, the implementation of clustering redundant tokens prior to merging minimizes information confusion, yielding additional gains of 0.3% and 0.4% in these respective areas. Through the incorporation of the visual-modality token compression module, the model’s instruction-following capability demonstrates an overall improvement of up to 5.6%.

Effect of Different Text-to-Image Focus Scores in Cross-Modality Attention Inhibition. Through comprehensive experimentation, we demonstrate the effects of utilizing various text-to-image focus scores as presented in Table 5. Initially, only text-to-image attention is employed to measure the text-to-image focus score. The implementation of

LLP	LWP	MG	CLST	GQA	TQA	MME	IF
✗	✗	✗	✗	61.9	58.1	1518.5	38.6
✓				60.2	57.2	1497.9	42.1
	✓			60.9	57.4	1509.9	43.5
	✓	✓		61.3	57.5	1512.1	<u>43.9</u>
	✓	✓	✓	<u>61.6</u>	<u>57.8</u>	<u>1515.8</u>	44.2

Table 4: Ablation Study on VMTC Stages. LLP represents Last Layer Pruning; LWP represents Layerwise Pruning; MG represents Merging; CLST represents Clustering.

Method	GQA	TQA	MME	IF
No CMAI	61.66	57.9	1508.9	39.9
+ TIA	61.31	57.3	1513.6	40.5
+ Sum TIA	61.42	57.6	1518.8	<u>42.9</u>
+ Discounted Sum TIA	61.05	57.2	1504.6	41.1
Ours	<u>61.57</u>	<u>57.8</u>	<u>1515.8</u>	44.2

Table 5: Ablation study of different text-to-image focus scores in Cross Modality Attention Inhibition(CMAI).

this method does not result in a significant performance decrease; however, it only yields a marginal 0.6% enhancement in the model’s instruction-following capability. To effectively suppress erroneous text-image token relations, it is imperative to consider text-to-image attention from other text tokens. In order to further validate the efficacy of our approach, we compare two straightforward alternatives. The first involves directly summing all text-to-image attentions as text-to-image focus score. Although this approach results in minimal performance degradation and a notable 3.0% improvement in instruction-following, it is not deemed the optimal design choice. The second alternative employs a discounted sum which multiplies each text-to-image attention by powers of a discount factor based on distance to the given token within the sentence. This method, leads to a significant performance decline attributed to the presence of long-distance attention within the sentence. Ultimately, our proposed method assigns different weights to various text tokens, thereby more effectively identifying and suppressing redundant text-image token relations. This approach achieves minimal performance loss while maximizing the enhancement in instruction-following capability, reaching up to 4.3%.

Conclusion

This research introduces a novel approach to study the instruction-following capability of MLLMs from a model-centric perspective instead of a data-centric one, providing insights into interactive adaptability. Experiments show that image redundancy significantly diminishes the instruction-following capability of MLLMs. To address this issue, we propose two strategies: visual-modality token compression and cross-modality attention inhibition, which are designed to condense redundant image tokens and focus the model's attention on key visual information. These two strategies result in a substantial enhancement of MLLMs' instruction-following capability while maintaining multimodal understanding performance comparable to SOTA models.

References

- Achiam, J.; Adler, S.; Agarwal, S.; Ahmad, L.; Akkaya, I.; Aleman, F. L.; Almeida, D.; Altenschmidt, J.; Altman, S.; Anadkat, S.; et al. 2023. Gpt-4 technical report. *arXiv preprint arXiv:2303.08774*.
- Alayrac, J.-B.; Donahue, J.; Luc, P.; Miech, A.; Barr, I.; Hasson, Y.; Lenc, K.; Mensch, A.; Millican, K.; Reynolds, M.; et al. 2022. Flamingo: a visual language model for few-shot learning. *Advances in Neural Information Processing Systems*, 35: 23716–23736.
- Bai, J.; Bai, S.; Chu, Y.; Cui, Z.; Dang, K.; Deng, X.; Fan, Y.; Ge, W.; Han, Y.; Huang, F.; et al. 2023. Qwen technical report. *arXiv preprint arXiv:2309.16609*.
- Bolya, D.; Fu, C.-Y.; Dai, X.; Zhang, P.; Feichtenhofer, C.; and Hoffman, J. 2023. Token Merging: Your ViT but Faster. In *International Conference on Learning Representations*.
- Cao, J.; Ye, P.; Li, S.; Yu, C.; Tang, Y.; Lu, J.; and Chen, T. 2024. MADTP: Multimodal Alignment-Guided Dynamic Token Pruning for Accelerating Vision-Language Transformer. In *Proceedings of the IEEE/CVF Conference on Computer Vision and Pattern Recognition*, 15710–15719.
- Cao, Q.; Paranjape, B.; and Hajishirzi, H. 2023. PuMer: Pruning and Merging Tokens for Efficient Vision Language Models. *arXiv preprint arXiv:2305.17530*.
- Chang, Y.; Wang, X.; Wang, J.; Wu, Y.; Yang, L.; Zhu, K.; Chen, H.; Yi, X.; Wang, C.; Wang, Y.; et al. 2023. A survey on evaluation of large language models. *ACM Transactions on Intelligent Systems and Technology*.
- Chen, J.; Zhu, D.; Shen, X.; Li, X.; Liu, Z.; Zhang, P.; Krishnamoorthi, R.; Chandra, V.; Xiong, Y.; and Elhoseiny, M. 2023a. Minigpt-v2: large language model as a unified interface for vision-language multi-task learning. *arXiv preprint arXiv:2310.09478*.
- Chen, K.; Zhang, Z.; Zeng, W.; Zhang, R.; Zhu, F.; and Zhao, R. 2023b. Shikra: Unleashing multimodal llm's referential dialogue magic. *arXiv preprint arXiv:2306.15195*.
- Chiang, W.-L.; Li, Z.; Lin, Z.; Sheng, Y.; Wu, Z.; Zhang, H.; Zheng, L.; Zhuang, S.; Zhuang, Y.; Gonzalez, J. E.; et al. 2023. Vicuna: An open-source chatbot impressing gpt-4 with 90%* chatgpt quality. See <https://vicuna.lmsys.org> (accessed 14 April 2023), 2(3): 6.
- Chu, X.; Qiao, L.; Zhang, X.; Xu, S.; Wei, F.; Yang, Y.; Sun, X.; Hu, Y.; Lin, X.; Zhang, B.; et al. 2024. Mobilevlm v2: Faster and stronger baseline for vision language model. *arXiv preprint arXiv:2402.03766*.
- Dai, W.; Li, J.; Li, D.; Tiong, A.; Zhao, J.; Wang, W.; Li, B.; Fung, P.; and Hoi, S. 2023. InstructBLIP: Towards General-purpose Vision-Language Models with Instruction Tuning. In *Advances in Neural Information Processing Systems*, volume 36.
- Dosovitskiy, A.; Beyer, L.; Kolesnikov, A.; Weissenborn, D.; Zhai, X.; Unterthiner, T.; Dehghani, M.; Minderer, M.; Heigold, G.; Gelly, S.; et al. 2020. An image is worth 16x16 words: Transformers for image recognition at scale. *arXiv preprint arXiv:2010.11929*.
- Fu, C.; Chen, P.; Shen, Y.; Qin, Y.; Zhang, M.; Lin, X.; Yang, J.; Zheng, X.; Li, K.; Sun, X.; Wu, Y.; and Ji, R. 2024. MME: A Comprehensive Evaluation Benchmark for Multimodal Large Language Models. *arXiv:2306.13394*.
- Goyal, Y.; Khot, T.; Summers-Stay, D.; Batra, D.; and Parikh, D. 2017. Making the v in vqa matter: Elevating the role of image understanding in visual question answering. In *Proceedings of the IEEE conference on computer vision and pattern recognition*, 6904–6913.
- Han, S.; Kelly, E.; Nikou, S.; and Svee, E.-O. 2022. Aligning artificial intelligence with human values: reflections from a phenomenological perspective. *AI & SOCIETY*, 1–13.
- He, K.; Chen, X.; Xie, S.; Li, Y.; Dollár, P.; and Girshick, R. 2022. Masked autoencoders are scalable vision learners. In *Proceedings of the IEEE/CVF conference on computer vision and pattern recognition*, 16000–16009.
- Hendrycks, D.; and Gimpel, K. 2016. Gaussian error linear units (gelus). *arXiv preprint arXiv:1606.08415*.
- Hudson, D. A.; and Manning, C. D. 2019. Gqa: A new dataset for real-world visual reasoning and compositional question answering. In *Proceedings of the IEEE/CVF conference on computer vision and pattern recognition*, 6700–6709.
- IDEFICS. 2023. Introducing IDEFICS: An Open Reproduction of State-of-the-Art Visual Language Model. <https://huggingface.co/blog/idefics>.
- Ji, J.; Qiu, T.; Chen, B.; Zhang, B.; Lou, H.; Wang, K.; Duan, Y.; He, Z.; Zhou, J.; Zhang, Z.; et al. 2023. Ai alignment: A comprehensive survey. *arXiv preprint arXiv:2310.19852*.
- Katz, D. M.; Bommarito, M. J.; Gao, S.; and Arredondo, P. 2024. Gpt-4 passes the bar exam. *Philosophical Transactions of the Royal Society A*, 382(2270): 20230254.
- Kim, W.; Choi, C.; Lee, W.; and Rhee, W. 2024. An image grid can be worth a video: Zero-shot video question answering using a vlm. *arXiv preprint arXiv:2403.18406*.
- Koubaa, A. 2023. GPT-4 vs. GPT-3.5: A concise showdown.
- Li, B.; Zhang, P.; Yang, J.; Zhang, Y.; Pu, F.; and Liu, Z. 2023a. Otterhd: A high-resolution multi-modality model. *arXiv preprint arXiv:2311.04219*.
- Li, J.; Li, D.; Savarese, S.; and Hoi, S. 2023b. Blip-2: Bootstrapping language-image pre-training with frozen image encoders and large language models. *arXiv preprint arXiv:2301.12597*.

- Li, J.; Li, D.; Xiong, C.; and Hoi, S. 2022. Blip: Bootstrapping language-image pre-training for unified vision-language understanding and generation. In *International Conference on Machine Learning*, 12888–12900. PMLR.
- Li, K.; He, Y.; Wang, Y.; Li, Y.; Wang, W.; Luo, P.; Wang, Y.; Wang, L.; and Qiao, Y. 2023c. Videochat: Chat-centric video understanding. *arXiv preprint arXiv:2305.06355*.
- Lin, B.; Zhu, B.; Ye, Y.; Ning, M.; Jin, P.; and Yuan, L. 2023a. Video-llava: Learning united visual representation by alignment before projection. *arXiv preprint arXiv:2311.10122*.
- Lin, Z.; Liu, C.; Zhang, R.; Gao, P.; Qiu, L.; Xiao, H.; Qiu, H.; Lin, C.; Shao, W.; Chen, K.; et al. 2023b. Sphinx: The joint mixing of weights, tasks, and visual embeddings for multi-modal large language models. *arXiv preprint arXiv:2311.07575*.
- Liu, H.; Li, C.; Li, Y.; and Lee, Y. J. 2024a. Improved baselines with visual instruction tuning. In *Proceedings of the IEEE/CVF Conference on Computer Vision and Pattern Recognition*, 26296–26306.
- Liu, H.; Li, C.; Wu, Q.; and Lee, Y. J. 2024b. Visual instruction tuning. *Advances in neural information processing systems*, 36.
- Liu, Y.; Duan, H.; Zhang, Y.; Li, B.; Zhang, S.; Zhao, W.; Yuan, Y.; Wang, J.; He, C.; Liu, Z.; et al. 2023a. Mmbench: Is your multi-modal model an all-around player? *arXiv preprint arXiv:2307.06281*.
- Liu, Y.; Iter, D.; Xu, Y.; Wang, S.; Xu, R.; and Zhu, C. 2023b. Gpteval: Nlg evaluation using gpt-4 with better human alignment. *arXiv preprint arXiv:2303.16634*.
- Luo, R.; Zhao, Z.; Yang, M.; Dong, J.; Qiu, M.; Lu, P.; Wang, T.; and Wei, Z. 2023. Valley: Video Assistant with Large Language model Enhanced ability. *arXiv preprint arXiv:2306.07207*.
- OpenAI. 2023. GPT-4V(ision) System Card. https://cdn.openai.com/papers/GPTV_System_Card.pdf.
- Ouyang, L.; Wu, J.; Jiang, X.; Almeida, D.; Wainwright, C.; Mishkin, P.; Zhang, C.; Agarwal, S.; Slama, K.; Ray, A.; et al. 2022. Training language models to follow instructions with human feedback. *Advances in Neural Information Processing Systems*, 35: 27730–27744.
- Radford, A.; Kim, J. W.; Hallacy, C.; Ramesh, A.; Goh, G.; Agarwal, S.; Sastry, G.; Askell, A.; Mishkin, P.; Clark, J.; et al. 2021. Learning transferable visual models from natural language supervision. In *International conference on machine learning*, 8748–8763. PMLR.
- Rao, Y.; Zhao, W.; Liu, B.; Lu, J.; Zhou, J.; and Hsieh, C.-J. 2021. Dynamicvit: Efficient vision transformers with dynamic token sparsification. *Advances in neural information processing systems*, 34: 13937–13949.
- Shang, Y.; Cai, M.; Xu, B.; Lee, Y. J.; and Yan, Y. 2024. Llava-prunmerge: Adaptive token reduction for efficient large multimodal models. *arXiv preprint arXiv:2403.15388*.
- Singh, A.; Natarajan, V.; Shah, M.; Jiang, Y.; Chen, X.; Batra, D.; Parikh, D.; and Rohrbach, M. 2019. Towards vqa models that can read. In *Proceedings of the IEEE/CVF conference on computer vision and pattern recognition*, 8317–8326.
- Taori, R.; Gulrajani, I.; Zhang, T.; Dubois, Y.; Li, X.; Guestrin, C.; Liang, P.; and Hashimoto, T. B. 2023. Stanford Alpaca: An Instruction-following LLaMA model. https://github.com/tatsu-lab/stanford_alpaca.
- Touvron, H.; Lavril, T.; Izacard, G.; Martinet, X.; Lachaux, M.-A.; Lacroix, T.; Rozière, B.; Goyal, N.; Hambro, E.; Azhar, F.; et al. 2023a. Llama: Open and efficient foundation language models. *arXiv preprint arXiv:2302.13971*.
- Touvron, H.; Martin, L.; Stone, K.; Albert, P.; Almahairi, A.; Babaei, Y.; Bashlykov, N.; Batra, S.; Bhargava, P.; Bhosale, S.; et al. 2023b. Llama 2: Open foundation and fine-tuned chat models. *arXiv preprint arXiv:2307.09288*.
- Vaswani, A. 2017. Attention is all you need. *arXiv preprint arXiv:1706.03762*.
- Wang, Z.; Chen, J.; Zhou, W.; Zhu, H.; Liang, J.; Shan, L.; Liu, M.; Xu, D.; Yang, Q.; and Qin, B. 2023. SmartTrim: Adaptive Tokens and Attention Pruning for Efficient Vision-Language Models. *arXiv preprint arXiv:2305.15033*.
- Wei, S.; Ye, T.; Zhang, S.; Tang, Y.; and Liang, J. 2023. Joint Token Pruning and Squeezing Towards More Aggressive Compression of Vision Transformers. In *Proceedings of the IEEE/CVF Conference on Computer Vision and Pattern Recognition*, 2092–2101.
- Wettig, A.; Gao, T.; Zhong, Z.; and Chen, D. 2022. Should you mask 15% in masked language modeling? *arXiv preprint arXiv:2202.08005*.
- Xu, R.; Yao, Y.; Guo, Z.; Cui, J.; Ni, Z.; Ge, C.; Chua, T.-S.; Liu, Z.; Sun, M.; and Huang, G. 2024. Llava-uhd: an lmm perceiving any aspect ratio and high-resolution images. *arXiv preprint arXiv:2403.11703*.
- Yu, T.; Yao, Y.; Zhang, H.; He, T.; Han, Y.; Cui, G.; Hu, J.; Liu, Z.; Zheng, H.-T.; Sun, M.; et al. 2024. Rllm-v: Towards trustworthy mllms via behavior alignment from fine-grained correctional human feedback. In *Proceedings of the IEEE/CVF Conference on Computer Vision and Pattern Recognition*, 13807–13816.
- Zheng, L.; Chiang, W.-L.; Sheng, Y.; Zhuang, S.; Wu, Z.; Zhuang, Y.; Lin, Z.; Li, Z.; Li, D.; Xing, E.; et al. 2024. Judging llm-as-a-judge with mt-bench and chatbot arena. *Advances in Neural Information Processing Systems*, 36.
- Zhou, J.; Lu, T.; Mishra, S.; Brahma, S.; Basu, S.; Luan, Y.; Zhou, D.; and Hou, L. 2023. Instruction-following evaluation for large language models. *arXiv preprint arXiv:2311.07911*.